H. S. Govinda Ram

WTL Report No. 78-1

February, 1978

COMPARATIVE CAVITATION INCEPTION STUDIES ON A HEMISPHERICALLY NOSED BODY

By

VIJAY H. ARAKERI AND H. S. GOVINDA RAM

DIVISION OF MECHANICAL SCIENCES
Department of Civil Engineering
Indian Institute of Science
Bangalore-560 012

WTL Report No. 78-1

February, 1978

COMPARATIVE CAVITATION INCEPTION STUDIES ON A HEMISPHERICALLY NOSED BODY

By

VIJAY H. ARAKERI AND H. S. GOVINDA RAM

This work was supported by the internal funds of the Civil Engineering Department

DIVISION OF MECHANICAL SCIENCES
Department of Civil Engineering
Indian Institute of Science
Bangalore-560 012

ACKNOWLEDGEMENTS

The financial support for the design, fabrication and installation of the 381 mm (15 inch) closed jet High Speed Water Tunnel facility was given by the Central Board of Irrigation and Power, Government of India. The financial grant for constructing the building to house the water tunnel facility was provided by the University Grants Commission, Government of India. This assistance from both the agencies is gratefully acknowledged. The authors would like to thank Professor N.S. Lakshmana Rao for his continued support at all times and they would also like to thank Mr. V. Ramarajan for his assistance in conducting the experiments. In addition, the authors would like to express their appreciation to the members of the Cavitation group for their helpful suggestions and the reviewers of the report for their constructive criticism.

ABSTRACT

Cavitation inception studies were conducted on an axisymmetric headform with a hemispherical nose. The test body with a diameter of 48.3 mm was mounted in the 381 mm axisymmetric test section of the Indian Institute of Science High Speed water tunnel facility. The Reynolds number range covered by the tests was from 4.8×10^5 to 8.6×10^5. Within this [Reynolds number] range good agreement was found between the present observations and those made previously on a similar test body at the California Institute of Technology and at the Pennsylvania State University Water Tunnel Facilities.

4.8×10^5 to 8.6×10^5
D = 48.3mm
V = 60/3.28 M/s
$\nu = 1.9 \times 10^{-6}$
at 28°C

TABLE OF CONTENTS

I INTRODUCTION

1 Background : Cavitation may be described as formation of inhomogenities in an otherwise homogeneous body of liquid due to dynamic reduction of pressures. The inhomogenities are in the form of macroscopic cavities containing either vapour of the liquid or a permanent gas which initially is in the form of a dissolved impurity in the liquid. Thus, formation of cavities containing primarily the vapour of the liquid is termed as "Vaporous" cavitation, whereas, formation of cavities containing primarily a permanent gas is termed as "gaseous" cavitation. A distinction between the two may be made from observations that vaporous cavities grow and collapse within a matter of milliseconds. On the other hand, gaseous cavities grow and collapse with time scales generally of the order of seconds. It is now recognised that it is the violent collapse of vapourous cavities which results in material damage commonly associated with cavitation.

Hydrodynamically one may divide the flow of a liquid around a solid body into three regimes. (i) In non-cavitating flow, the liquid follows the classical hydrodynamic laws for an incompressible fluid. (ii) In what may be called limited or incipient cavitation, small discrete bubbles or areas occupied by patches of gas or vapour first appear. (iii) Fully cavitating or super-cavitating flow is characterized by a single large vapour or gas cavity enveloping some portion of the body. Occurrence of cavitation is a possibility in devices which involve liquid flows either at high velocities and/or at reduced pressures. Some examples of such devices are : ship propellers, hydraulic machineries, valves, torpedoes, lubrication bearings etc. In all applications, occurrence of cavitation is an undesirable phenomenon since it results in the reduction of efficiency or increase in the drag, severe vibrations, material damage and production of intense high frequency noise.

2 Some physical aspects of cavitation : Since the inception of cavitation distinguishes the limit for cavitation - free operation it has been the subject of considerable experimental and theoretical research. Theoretical predictions indicate that pure homogeneous liquids can withstand significant amount of tensile stresses (or negative pressures) of the order of thousands of atmospheres. However, so far carefully treated liquid samples are known to withstand only moderate tensile stresses of the order of hundreds of atmospheres[1]. The reason for this discrepancy has led to the postulation of presence of impurities in the liquid environment commonly known as "nuclei". It is apparent that in considering flows about a submerged body the nuclei or weak spots can come from two sources ; namely, from within the free stream and from the surface of the test body itself. Nuclei of the first type are termed as "stream nuclei" and the latter as "surface nuclei". The physical nature of the free stream nuclei have been hypothesized to be of the form of free gas bubbles, gas trapped in the crevices of solid particles, or solid partiels themselves which are present in the fluid. It has been suggested that surface nuclei consist of gas trapped in microscopic crevices of the body surface. In any case the presence of nuclei plays a fundamental role in the inception process.

Whatever may be the source of these weak spots, finally cavitation occurs as a result of vaporous or gaseous growth of these nuclei into visible cavities. The ability of the available nucleus to grow to a visible size would definitely be influenced by the magnitude and duration of the low pressures experienced by the nucleus. Vaporous growth would be possible only if the nucleus' experiences pressures which are either equal to or below the vapor pressure of the liquid. Gaseous growth is possible

at any pressures. However, the liquid should be supersaturated with a permanent gas with respect to the gas content of the nuclei. The growth once started will in addition be influenced by whether the nucleus travels along with the fluid outside the boundary layer or by whether it is enterained within the boundary layer. In the latter case the nucleus then may experience zones of boundary layer transition, turbulence and separation if existing. These real fluid features virtually make it impossible to analytically predict the growth pattern of a cavitation nucleus or bubble subject to boundary layer effects. On the other hand, in the absence of boundary layer effects the growth pattern of a cavitation nucleus or bubble can be predicted quite accurately by analytical means[2]. However, in most practical situations the neglect of real fluid effects can be totally unjustified.

3 Role of Water tunnels in Cavitation research : Due to the complex nature of the cavitation inception process it has been common engineering practice to resort to model testing to predict the onset of cavitation in prototype situations. The tool to carry out the model testing has been the water tunnel which essentially is an analog of a wind tunnel. In a water tunnel provision is made to control the test section pressure independent of the test section velocity. This is an essential feature of a water tunnel where cavitation model testing is conducted. From the results of model testing, prototype predictions are based on the use of proper similarity laws. One of the important similarity parameters found to characterize cavitating flows has been the cavitation number σ , defined as

$$\sigma = \frac{P_\infty - P_v}{\frac{1}{2} \rho V_\infty^2}$$

where, P_∞ is the static pressure and V_∞ the free stream velocity some distance away from the model. ρ is the liquid density and P_v is the vapour pressure at the bulk temperature. The magnitude of σ , as inception of cavitation is approached from non-cavitating conditions is commonly denoted by σ_i and termed as 'incipient cavitation index'. On the other hand, the magnitude of σ as disappearence of cavitation is approached from cavitating conditions is commonly denoted by σ_d and termed as 'desinent cavitation index'. It has been found experimentally that σ_i and σ_d are not always equal to each other for identical model tests indicating hysteresis effects.

If σ was the only important parameter then the similarity or the scaling law to predict the onset of cavitation in prototype situations from model tests would simply be that, σ_i = constant. However, tests have shown that even for certain simple shaped geometrically similar bodies, σ_i is not equal to a constant but is a function of body size, free stream velocity, air content and nuclei content of water etc. This dependence of σ_i on other parameters for geometrically similar bodies is commonly termed as "scale effects". Thus, water tunnels have not only been used for model testing but also to study the scale effects using certain 'simple' bodies. Such studies have been used to identify other important scaling parameters besides the cavitation number. The success so far has been encouraging but not satisfactory.

4 Some Cavitation scaling laws : Under the simplest of assumptions, namely that cavitation appears as soon as liquid pressure at any point is reduced to the vapour pressure, one gets the relationship

$$\sigma_i = - C_{p\ min}$$

where, $C_{p\,min}$ is the minimum pressure coefficient of the body-liquid system. This rule has been used quite extensively by design engineers to predict the onset of cavitation in prototype situations with a good degree of success. However, it is ironical that laboratory tests on simple shaped bodies for which the magnitude of $C_{p\,min}$ is known, have shown that σ_i can differ significantly from the negative value of the minimum pressure coefficient. The reasons for the descrepancy have only been recently[3] traced partly to the nature of the viscous flow past the test body. For example, with the presence of laminar separation, σ_i was found to correlate well with the negative value of the pressure coefficient at the location of laminar separation, $-C_{ps}$ rather than $-C_{pmin}$. Similarly for flows with attached boundary layers σ_i was found to correlate well with the negative value of the pressure coefficient at the location of turbulent transition, $-C_{ptr}$ rather than $-C_{pmin}$. At high Reynolds numbers, typical of prototype conditions, turbulent transition will approach the minimum pressure point which means that $-C_{ptr}$ and $-C_{pmin}$ may not differ greatly under these circumstances. It is perhaps for this reason that better agreement between σ_i and $-C_{pmin}$ has been found for the prototype conditions than for the laboratory situations. However, it must be emphasized that either determining the viscous flow regimes or the magnitudes of $-C_{ps}$, $-C_{ptr}$ and $-C_{pmin}$ for complex fluid flows, typical of prototype conditions, may not be a simple task. This again forces one to resort to model testing in order to predict the magnitude of σ_i.

5 Scope of present work : As noted previously water tunnel facilities can be useful tools to conduct cavitation studies under controlled conditions. In India, primarily two water tunnel circuits are available for such studies. One is located at the Central Water and Power Research Station (CWPRS), Khadekwasla, Poona and has been used quite extensively for model testing of hydraulic machinery. The second one is located at the Indian Institute of Science (IISc), Bangalore and is particularly suited for conducting both applied and basic research in cavitation. In addition, the IISc circuit is readily suitable for conducting model testing of underwater projectiles and also can easily be adapted for model testing of other prototype devices like marine propeller, hydraulic valves, etc. It is the purpose of the present work to demonstrate the feasibility of the IISc water tunnel for conducting cavitation studies. It was feld that the best way to accomplish this would be by conducting cavitation studies on a test body whose inception characteristics have been well documented. It is for this reason that a hemispherical-nosed body the inception characteristics of which have been studied quite extensively was chosen for the present study.

The text of the report describes the present experimental study including the experimental methods, discussion of results followed by a summary. Very few details of the facility itself are contained in the text; however, a brief description of the facility for interested readers is provided in an appendix.

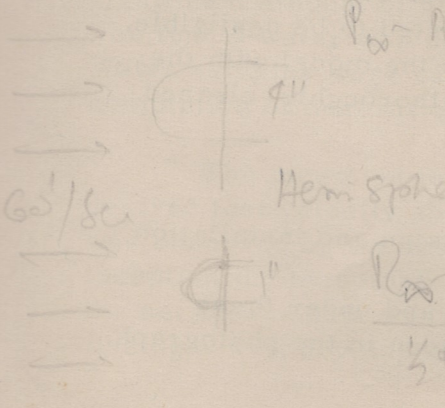

II EXPERIMENTAL METHODS

1 Test facility : - The experiments described were conducted in the Indian Institute of Science (I.I.Sc.) High Speed Water Tunnel[+] (HSWT). Only few pertinent details concerning this facility will be provided in this section.

The basic flow circuit is illustrated in figure 1. It consists of the usual features of a wind or water tunnel. However, the present facility is, in addition, equipped with a resorber which is a common feature of some of the water tunnel facilities located elsewhere but not all of them. The primary purpose of a resorber is to dissolve back into solution any air bubbles which are generated either due to cavitation and or due to the degassing process in the low pressure regions of the flow circuit. The dissolution is accomplished by subjecting the air bubbles to high pressures for sufficiently long periods of time in the resorber. Thus, normally the resorber is located in the bottom leg of the flow circuit immediately downstream of the pump. Another prominent feature of the present test facility is its large contraction ratio between the settling chamber and the test section. A similar contraction ratio at the CIT facility has resulted in excellent flow qualities in the test section and in addition to reduced free stream turbulence level as compared to other facilities having smaller contraction ratios.

The maximum attainable velocity in the test section and the pressure control range of the present facility is comparable with other similar facilities located elsewhere (see table 1). To attain maximum velocity noted in table 1 the system has to be pressurized to almost seven atmospheres to avoid cavitation in the test section. However, this has not been possible due to leakage problems and the maximum velocity attained so far with bare test section has been of the order of 18m/s (60 fps). The lowest pressure attainable in the test section was also limited by the capacity of the available vaccum pump. This limited the lowest test velocity at which cavitation tests could be conducted to about 9m/s (30 fps). With leakages taken care of and with other improvements the test velocity range could certainly be increased.

2 Test Model : The test model chosen for the present work is an axisymmetric headform with a hemispherical nose and a cylindrical after body, shown in figure 2. The contour of the test model was examined with an optical projection equipment available at the National Aeronautical Laboratory. The actual contour was compared with a 10X drawing of the true contour. This comparison showed that the actual contour was within 50 microns (0.002") of the true contour. The headform was mounted by a single strut element firmly secured to the top window of the test section. Figure (3)(a) shows a photograph of the headform in the test section under supercavitating[++] conditions. The test model occupied only about 1.6 percent of the through flow area. Therefore, the blockage effects are expected to be negligible. During mounting of the headform proper care was taken to allign the model with the centre line of the test section. The nose of the model was also thoroughly cleaned with carbon tetrachloride prior to mounting in the test section.

+ See refs. (4, 5, 6) for description of this facility during its design and installation periods.

++ supercavitating means a large cavity is formed on the model and under these conditions normally the strut element also cavitates as seen in the photograph.

3 General experimental techniques : The velocity in the test section was computed by measuring the pressure drop across the contraction cone by a mercury - water manometer. By knowing the area ratio one can compute the velocity from the measured pressure drop by applying the Bernoulli equation. It is known from literature that for facilities of the present type velocity measurements by the above technique are quite accurate even with neglect of viscous corrections. The test section static pressure was measured with a differential mercury manometer with one end open to the atmosphere. The pressure tap for this measurement was located about fourteen diameters from the model nose. In principle, due to the boundary layer growth along the tunnel walls proper calibration is required to infer the magnitude of the tunnel static pressure close to the model for the computation of cavitation number and free stream velocity. However, again from past measurements[7] it is known that these corrections are generally only of the order of a few percent and therefore they were not accounted for in the present computations.

Since, the present tunnel facility is not equipped with a cooling device it was necessary to check if the water temperature altered significantly during continuous operation. However, it was found that due to the large volume of water involved in the circuit the temperature rise was only of the order of 1°C for continuous operation of about six hours at present test velocities. The temperature was measured with a mercury thermometer located at the top of the vertical leg of the tunnel circuit near the settling chamber.

The single flash photographs of cavitation were obtained by using the stroboscope PR 9107 and flash torch 9117 B/03 made by M/s Phillips. At maximum intensity settling the flash duration at fifty percent of amplitude is about 15 μS. This duration was short enough to "freeze" any motion possible even at the highest test velocities.

The air content of the tunnel water was inferred from directly measuring the dissolved oxygen content of the water sample by a simple titration technique.

4 General experimental procedure : To begin the experiments, the normal procedure was to fill the tunnel with fresh supply of filtered water. During filling proper care was taken to open all the vents at high points to remove trapped air pockets. Then the water was deaerated by running the tunnel with a test section velocity of about 9m/s and a test section pressure reduced to its lowest possible value. This resulted in supercavitation on the model-strut system and also some cavitation in the diffuser section could be heard. The tunnel was left running in the above state continuously for almost half an hour. Then the flow was stopped and after waiting for a few minutes the system was pressurized and air vents at all the high points were opened. Since the present facility is equipped with a horizontal resorber it was observed that significant amount of air would come out of solution at the high points of the resorber. The tunnel water was deaerated by this technique for almost three hours continuously. Water samples were carefully drawn just prior to commencement and also just after completion of deaeration for air content measurements.

The inception tests were conducted by increasing the tunnel velocity to the desired test velocity and then the tunnel pressure was slowly reduced until cavitation was observed on the test model under stroboscopic light illumination. At the point of inception the manometer values were closed to "freeze" the readings and immediately the necessary data was recorded. The desinent tests were conducted by first establishing a well developed cavity on the model and then the tunnel pressure was slowly

increased till the last traces of cavitation on the model disappeared. After each inception or desinent test the tunnel was run at high pressures (about two atmospheres absolute in the settling chamber) for almost two minutes. Also each time a new test velocity was reached the tunnel was run at similar high pressures for five to six minutes.

Both at the start and at the end of cavitation tests, the temperatures and barometric readings were noted down.

III RESULTS AND DISCUSSION

1 Inception observations : Due to the presence of the resorber in the present facility very few or no microscopic air bubbles could be observed in the flow upstream of the model under stroboscopic light illumination. This was found to be the case even at low test section pressures indicating that the resorber was quite effective for what it was intended. Occasionally when a new test velocity was reached, a large number of macroscopic free stream air bubbles could be observed; however, these would slowly disappear after the tunnel was run at high pressures for a few minutes. Under no circumstances, inception tests were conducted in the presence of a copious supply of macroscopic free stream air bubbles. However, under stroboscopic illumination it was clear that plenty of macroscopic dirt particles including paint chips were present in the flow. Whether this had any effect on the inception observations cannot be ascertained at this point.

As the tunnel pressure was reduced, cavitation at inception appeared suddenly and was in the form of a ring of bubbles around the headform. A photograph of this type of cavitation is shown in Figure 3(b). The bubble type of inception just noted took place at all the test velocities except for the lowest ones of about 10m/s. At the lower velocities, the extent of cavitation at inception was more developed similar to cavitation observed in the photograph of figure 3(c). This type of cavitation is commonly termed as "band" type of inception. These present observations are entirely consistent with inception observations on a hemispherical nosed body at the CIT High Speed Water Tunnel[3].

During inception studies it was noted that at test velocities of around 12m/s and 14.5m/s the tunnel operating floor was vibrating either continuously or in spurts. Since the test section is directly connected to the operating floor it was expected that the vibrations would be carried over to the model itself. Close visual observations under stroboscopic lighting clearly indicated that the test body was vibrating at these test velocities. However, the type of cavitation at inception observed at these velocities was not found to be any different than the type of cavitation at inception observed for other test velocities when the floor vibrations were not present. Whether inception measurements themselves were affected by these events is not known.

2 Inception Measurements : Measured cavitation indices at inception on the present test body are shown in figure 4. As noted previously most of the data is for bubble type of inception except at the lowest velocity. Also shown in the same figure is the desinence data. Except at the lowest velocity very little difference between the incipient and desinent cavitation indices can be observed. At the lowest velocity the band type of attached cavities were observed to disappear very slowly indicating that air was going into solution from these attached cavities into the surrounding water. It is perhaps these events which result in the observed difference between the incipient and desinent cavitation index at the lowest velocity. In figure 4, the incipient data shown at a velocity of about 16m/s was taken with observations from two opposite side windows. Very little difference in the incipient indices was noted supporting the visual observations of symmetrical appearance of cavitation on the headform at inception.

In figure 5, present average inception measurements are compared with similar measurements made at the CIT and Ordance Research Laboratory facilities[8] on a 50.8 mm hemispherical-nosed body. It should be noted that present data agrees

very well with the previous data. However, it is clear that it would be useful to extend the present measurements over a wider range of Reynolds number. It may be pointed out that the CIT facility is equipped with a resorber whereas the ORL facility is not. As noted previously the present facility is equipped with a resorber and the good agreement between various measurements seen in figure 5 seems to indicate that at least the inception characteristics of the hemispherical nosed body are not influenced by the presence or absence of a resorber.

All of the σ_i values shown in figure 5 including the present measurements are significantly below the negative magnitude of the minimum pressure coefficient under noncavitating conditions for the hemispherical nosed body (see figure 6). As noted earlier it is common engineering practice to predict the onset conditions of cavitation by equating σ_i with $-C_{p\,min}$. The present measurements certainly indicate that this practice may lead to erroneous predictions even though for the hemispherical nosed body σ_i does approach $-C_{p\,min}$ with increase in Reynolds number. A recent study[3] has shown that at least for the hemispherical nosed body it may not even be proper to equate σ_i with $-C_{p\,min}$. The bubble type of inception seen in figure 3(b) has been found to be associated with the reattachment region of a laminar separation bubble. Whereas the smooth cavity seen in figure 3(c) has been found to be associated with the laminar separated region itself. Both laminar separation and reattachment are normally significantly downstream of the minimum pressure point. From these observations it was concluded that σ_i should strictly be equated to the negative magnitude of the pressure coefficient at laminar separation ($-C_{ps}$) on the body. Present measurements do indicate this trend in the sense that measured σ_i values are in closer agreement with $-C_{ps}$ value of about 0.65 than with the $-C_{p\,min}$ value of about 0.75.

3 Cavitation Photographs : Cavitation near incipient conditions is shown in the photograph of figure 3(b). With σ slightly below σ_i an attached cavity was formed with a smooth leading edge as seen in figure 3(c). With further reduction in cavitation number the cavity length increased as seen in the photographs of figures 3(d) and 3(e). It may be noted that with attached cavities down stream of detachment, cavity surface is "frothy" and bubbly. It is this region which is prone to cavitation damage if cavities persist for an extended time period. It is also this region which is very unsteady in characteristics and in addition is a source of intense high frequency noise.

At a given velocity, if the tunnel pressure is lowered to essentially the lowest possible value, then heavy cavitation results on the body-sturt system. At this point, the body is said to be supercavitating and a photograph illustrating this regime of cavitation is shown in figure 3(a). On the body a single large cavity is formed with a clear and smooth interface. In the photograph, the clarity is evident from the fact that the test body is visible through the cavity.

It may be pointed out here that physically the cavity surface is a constant pressure surface and also is a boundary of zero shear. Thus, a solid body designed as per cavity contour will not exhibit separation. Thus, studies of cavity contour under supercavitating conditions may be used to design low drag bodies.

IV SUMMARY

The present work has clearly demonstrated the feasibility of using the Indian Institute of Science high speed water tunnel for conducting cavitation studies. The tunnel performed quite satisfactorily during the tests and in particular, the resorber was found to be effective at all the test velocities and pressures. During cavitation tests none or very few macroscopic air bubbles were visible in the liquid approaching the model. This being the consequence of the provision of the resorber in the present facility.

On the hemispherical-nosed test body, cavitation at inception was in the form of a ring of bubbles situated slightly downstream of the tangent point. This was the case at all test velocities except the lowest ones when cavitation at inception was in more developed form with a clear attached leading edge. These observations and in addition the measured magnitude of cavitation index at inception during the present study are found to agree well with similar observations of cavitation inception on a hemispherical nose body conducted at the California Institute of Technology and the Pennsylvania State University water tunnel facilities. Present tests covered a Reynolds number range of 4.8×10^5 to 8.6×10^5 and within this Reynolds number range the magnitude of cavitation index was found to increase from 0.627 to 0.66 with increase in Reynolds number. The above noted inception cavitation indices are found to be significantly below the negative value of the minimum pressure coefficient of 0.75 for the test body under noncavitating conditions.

PREFACE TO THE APPENDIX

The Indian Institute of Science water tunnel facility was errected during the year 1964-1968 and is almost ten years old now. Copies of an earlier report describing the design aspects of the facility have been exhausted. Primarily for this reason a brief description of the water tunnel facility is provided in the Appendix of this report. An extensive report describing the various design and application features of the water tunnel facility in greater detail is under preparation.

V APPENDIX

The 381 mm (15 inch) closed jet High Speed Water Tunnel

A high speed water tunnel has become indispensable tool in the study of cavitation which is of common occurrence in devices which handle high speed liquid flows. Water tunnels have not only been used to conduct model studies of prototype situations but also to derive necessary scaling laws to predict the occurrence of cavitation in prototype conditions based on model testing. In addition, water tunnels have also been used to conduct basic studies in incipient and developed cavitation. In the future these studies may play an increasingly important role in evolving accurate designs of components which may be less prone to cavitation under otherwise identical situations. It would be a very limited point of view to imply here that water tunnels can be used exclusively for cavitation studies since they are being used for studying other hydrodynamic aspects of flow around solid bodies as well. Some of the differing physical properties of water as compared to air can also be exploited. For example, for a given body size and test section velocity, the Reynolds number in water flow will be about fifteen times the corresponding Reynolds number in air flow. In addition, for a given velocity the magnitude of the dynamic head[+] in water flow will be about 800 times the dynamic head in corresponding air flow. Thus, measurements of fluctuating pressures which are generally proportional to the dynamic head can be a much simpler task in the water medium than in the air medium. Besides the above two advantages, the fact that the index of refraction of water is a very sensitive function of temperature as compared to air can be usefully exploited for optical flow visualization techniques like the shadowgraph, schlieren and interferometry. In addition, water is an excellent medium for conducting flow visualization studies using non-optical techniques like the hydrogen bubble, dye injection and oil film methods.

Thus, a water tunnel can be a very useful facility to study many aspects of fluid flow problems. With this in mind a high speed water tunnel facility has been established at the Indian Institute of Science. The tunnel circuit is housed in a separate three floor reinforced cement concrete building. The approximate dimensions of the building are 40 metres in length, 20 metres in width and 20 metres in height. A photograph of the building is shown in figure 7(a). Some of the supporting units of the facility like the water filter plant, underground raw and clear water tanks and a step-down transformer used for the power supply to the main motor are located outside but adjacent to this building.

The present facility is a closed loop water tunnel circuit with an axisymmetric test section of 381 mm in diameter. A sketch of the tunnel circuit is shown in figure 1. Figure 7(b) shows a photograph of the upper leg of the tunnel. First the diffuser portion is seen followed by the test section, the contraction cone and finally the settling chamber. Also seen in the photograph above the settling chamber is the pressure control vessel marked as K in figure 1. Figure 7(c) shows a photograph of essentially half the resorber which is above the ground level. In the same figure the I-beam sections welded in a cross-hatched manner to strengthen the resorber side flat plate may also be seen. Figure 7(d) shows a photograph of the 600 horse power variable speed induction motor which drives the four bladed main circulating pump. The main power supply to the motor is connected through an oil circuit breaker and the rotational

---

[+] The dynamic head is given $\frac{1}{2} \rho V^2$, where ρ is the density of the fluid and V, the average velocity

speed of the motor is varied by a liquid regulator control and a photograph of both of these component is shown in figure 7(e). In this photograph the liquid regulator control unit is located nearside and on the far side is the oil circuit breaker. In the remaining portion of the appendix description is given of the following listed components and supporting equipments of the water tunnel facility :

1) Test Section
2) Transition pipe
3) Diffuser
4) Resorber
5) Contraction Cone
6) Flow correcting devices
7) Circulating pump and its drive
8) Speed and pressure control
9) Water treatment plant
10) Photographic accessories.

1 Test section : The present test section is that of a closed jet type with a constant inner diameter of 381 mm and an overall length of 1524 mm. Based on potential flow pressure distribution calculations+ on several axisymmetric bodies it can be shown that a test body of maximum diameter of 50 mm would experience essentially no blockage effects in the above sized test section. For larger sized bodies suitable blockage corrections would be necessary. An alternative technique of testing larger bodies would be to compute the shape of the streamlines at the location of the tunnel walls and then provide at the walls curved liners matching the computed shape of the streamline. This method of overcoming blockage effects has been used quite successfully at the Pennsylvania State University water tunnel facility for a number of years.

The test section is a gun-metal casting and is provided with four 914 mm x 254 mm transparent perspex windows for photographic and observational purposes. The windows are made of 127 mm perspex blocks with one side machined to match the 381 mm diameter of the test section and the other side left flat. Some geometrical details of the windows and the test section are shown in figure 8. The top perspex window can be substituted with a metal hatch cover which has provision for mounting a single bladed sting support. An exisymmetric test body can then be securely mounted to this sting support. The test section is also provided with ten static pressure tappings with a hole diameter of 4.76 mm. The first pressure tap is located at 90.5 mm from the beginning of the test section and subsequent ones are located with a regular spacing of 152.4 mm.

2 Transition pipe : A transition pipe of gun-metal casting with an uniform thickness of 19 mm is used to connect the test section and the diffuser in the upper leg of the tunnel. Its diameter at the inlet is 381 mm and at the outlet it is 405 mm. Its overall length is 457 mm. The wall surface is parabolic in shape and it joins smoothly with the corresponding slopes at the test section and diffuser ends.

+ These calculations were carried out by using the Donglas Newman programme by one of the authors during his stay at the California Institute of Technology.

3 Diffuser : The primary purpose of the diffuser is to slow down the high velocity fluid in the test section to lower values. This necessarily means increasing pressure along the diffuser and the dangers of possible separation under these circumstances are well known. The presence of separation means substantial increase in losses and also may lead to unsteady velocities in the test section. For these reasons the design of the diffuser has to be done with proper care. The guidelines followed in the design of the diffuser for the present tunnel circuit are based on the work of Robertson et.al[9].

The diffuser in the upper horizontal portion of the tunnel has an initial diameter of 405 mm and a final diameter of 889 mm with a divergence angle of 6°. The diffuser continues in the vertical leg after a 90° turn. The vertical portion has an initial diameter of 1054 mm and a final diameter of 1448 mm again with a divergence angle of 6°. The combined diffuser is made up of nine individual pipe sections which have been fabricated out of 12.7 mm M.S. plates. Suitably matching flanges are welded at the end of each pipe section and successive pipe sections are bolted together with a 3.18 mm rubber gasket placed between the flange sections.

4 Resorber : During cavitation studies the flowing liquid in a water tunnel is exposed to low pressures in the test section area. Under these circumstances air which is initially dissolved in the liquid can come out of solution in the form of macroscopic free air bubbles. If these air bubbles are not subjected to high pressures for sufficiently long time they will not go back into solution. As a consequence the liquid upstream of a model in the test section can have a copious supply of free macroscopic air bubbles. In some cases the presence of these bubbles can obscure the view of the test body. It can also influence the far field hydrodynamic or cavitation noise measurements and a recent study by Gates[10] has shown that it in addition can also affect the basic viscous flow past a test body. In addition, these bubbles can play a significant role as nucleation sites in cavitation inception studies.

At this juncture we will not debate as to whether the presence of these bubbles is a good or bad characteristic of a water tunnel with respect to prototype simulation experiments. However, it should be noted here that to remove the presence of these bubbles, an additional component in the tunnel circuit is required. The purpose of this additional component commonly termed "resorber" is to subject the macroscopic air bubbles created in the test section to high pressures for sufficiently long time to redissolve them into solution. Thus, the efficiency of a resorber is determined by the average static pressures and longer the residence time the better the effectiveness of a resorber. For this reason the resorber is normally located in the bottom leg of a tunnel circuit immediately downstream of the pump and the resorber volume is made as large as possible to increase the residence time.

In the past, several resorber designs have been incorporated in the water tunnel circuits[11]. One of the simplest design is to place the lower leg of the tunnel circuit significantly below ($\sim$ 60 meters) the centre line of the test section. The diameter of the lower leg is also made large as compared to the size of the test section. In alternative designs the lower leg is placed at lesser heights from the test section centre line but its length is made significantly longer than the minimum length possible. Perhaps the earliest facility to incorporate a resorber into its water tunnel circuit is located at the California Institute of Technology (CIT). The CIT resorber is in the form of a cylindrical tank of 3.54 meters diameter and 17.7 meters in length. The tank is buried in a pit immediately downstream of the pump with the bottom-most point of the resorber being 25.9 meters below the test section centre line. The residence time of

of bubbles is further increased by making a partition in the tank and therefore the fluid entering makes four passes within the resorber tank before leaving.

The CIT resorber over the years has proven to be a very effective design. However, the costs involved in deep excavations can be high and as a compromise the present resorber cylindrical tank is placed horizontally immediately downstream of the pump. The tank is 3.66 meters in diameter and has a length of 7.63 meters giving a resorber volume of 80.17 cubic meters. The bottom-most point of the resorber is 9.093 meters below the centre line of the test section. The location of the resorber with respect to other components of the tunnel circuit is illustrated in figure 1.

The resorber is fabricated out of 3640 x 1524 x 25 mm size mild steel plates. Three such plates bent into circular shape were welded to form a ring of width 1.524 meters and a diameter of 3.66 meters. Five such rings are joined together by welding to form the cylindrical section of the resorber. At the end of the cylindrical section, flat mild steel plates of 35 mm thickness are welded at the circumference. These end plates have suitable holes and flange connections for joining the inlet and outlet pipes. In addition, since the end plates would be subjected to large stresses under pressurized conditions they have been strengthened by welding I-beam sections in a cross hatched manner. The details of this are shown in figures 9 and 10 which also illustrate geometrical details of the resorber itself. To increase the residence time of a fluid in the resorber four baffle plates of semi-circular shape are welded to form openings at the top and bottom alternatively. The locations of the baffle plates are also shown in figure 9.

5 Contraction Cone : The fluid after leaving the resorber flows in constant diameter (1525 mm) pipe sections with two ninety degree elbows. After the second ninety degree elbow the fluid enters a relatively long settling chamber in the upper horizontal section. The relatively low velocities in the settling chamber are increased to the high test section velocities through a suitably designed contraction cone. The guidelines used in arriving at the shape of the contraction cone are based on the work of Thwaites[12]. The shape is such that the velocity increases monotonically and hence the pressure decreases continuously approaching the test section. The details regarding the shape of the present contraction cone are shown in figure 11. It may be seen that a contraction ratio of 16 is provided which is relatively high compared to most other water tunnel facilities.

The contraction cone is assembled from three separate 19.1 mm thick gunmetal castings. The individual sections are bolted together with 3.18 mm rubber gasket placed between the matching flanges. Internally the contraction cone was machine finished to the prescribed shape. At the centre line thirteen pressure tappings are provided with a nominal spacing of 150 mm. Besides these, the end flanges are tapped at four locations circumferentially with ninety degree separations. These can be connected together to form piezometric rings which can be used to measure pressure drop across the contraction cone.

6 Flow correcting devices : One of the functions of a water tunnel is to provide a steady stream of high velocity fluid with a uniform distribution across the test section. This can be achieved only by avoiding gross irregularities in the velocity distribution at sharp bends which are required in a recirculating facility. A common practice is to provide suitably designed guide vanes at the sharp bends.

In the present circuit guide vanes are provided at all the six ninety degree bends. One of the ninety degree bends is an integral part of the pump and the guide vanes for this bend were designed by the manufacturers of the pump. The guidelines followed in designing the turning vanes for the other bends were based on the works of Klein et. al[13] and Ripken[14]. The vane shape used in the present circuit bends is shown in figure 12. It has maximum thickness of 24.9 mm and a chord length of 137 mm. Twenty such vanes are provided at the first turn giving a spacing/chord ratio of 0.48. Thirty vanes have been provided at the remaining turns giving a spacing/chord ratio of about 0.48 also. The angle of attack when the vane is set such that the tangents drawn at the leading and trailing edges on the upper surface are parallel to the respective centre lines of the pipes is about 56°.

Even though gross irregularities in the velocity distribution can be minimized by using turning vanes at sharp bends smaller irregularities may still exist in the velocity distribution approaching the contraction cone. A large contraction ratio as provided in the present circuit may alleviate the irregularities in the test section but they may not be completely removed. Thus, additional flow corrective devices in the form of honeycombs or screens are necessary in the settling chamber. The present facility is equipped with a honeycomb having square cells measuring 25.4 mm x 25.4 mm and with an aspect ratio of five. The honeycomb is located in the settling chamber approximately three meters upstream of the beginning of the contraction cone.

7 Circulating pump and its drive : The present facility was designed to provide a maximum test section velocity of about 30.3 meters per sec. At this velocity the total head loss was estimated to be of the order of 10 meters. In addition, to avoid cavitation the pump R.P.M. at the maximum discharge should not be excessively high. To satisfy these requirements a four bladed, axial flow, propeller type pump was purchased from the Byron and Jackson Limited, Los Angles, U.S.A. Even though it is common practice to equip water tunnel circuits with a pump of pitch adjustable blades in view of availability and cost considerations a pump with fixed pitch blades was procured for the present facility.

The present pump is capable of delivering 210 cubic meters per minute at a total head of 10.5 meters. This is achieved at a pump R.P.M. of about 600 with an efficiency of 80 percent. It is clear that the pump meets the earlier noted requirements quite adequately. The characteristic curves of the pump used in the present tunnel circuit are provided in figure 13. The horse power required by the pump at the design point with an efficiency of 80 percent. works out to be about 625.

To match this pump requirement, a 600 horse power induction motor+ is connected to the pump shaft. The motor is of slip ring type with eight poles and when operated on 50 cps power has a synchronous speed of 750 R.P.M. However, speed variation is possible since the motor has a wound rotor.

8 Speed and pressure control : Presently the speed variation is achieved by connecting the rotor winding to an external liquid rheostat control+. One of the disadvantages of this type of control is the limited range (normally 2 : 1) within which the speed control is possible. The controller basically comprises of a tank containing three pairs of vertically moving electrodes and three pairs of fixed electrodes. A pair of fixed and moving electrodes are connected to each phase of the rotor circuit. The tank

---

+ supplied by the Associated Electrical Industries Limited, United Kingdom.

is filled with suitably concentrated electrolyte-water solution so that a resistance path is created between the electrodes. Thus, resistance variation is possible by varying the distance between the fixed and moving electrodes which are both immersed in the electrolyte-water solution. The starting or the minimum speed when the electrodes are separated at their maximum distance depends on the concentration of the electrolyte in the solution. For example, with essentially zero electrolyte concentration the minimum rotational speed was found to be about 50 R.P.M. During operation the electrolyte-water solution tends to get heated up due to power dissipation and for this reason a bank of tubes in the tank is provided through which cooling water is circulated. A spray type condenser unit is provided adjacent to the liquid rheostat control outside the water tunnel building which helps to maintain the cooling water temperature reasonably close to the room temperature level.

To conduct cavitation studies in a water tunnel it is not just sufficient to control the test section velocity but it is also necessary to control the operating static pressure independently. Normal technique of achieving this is to make the tunnel circuit a closed system and connect it to an air chamber which has a free surface in it. Thus by controlling the pressure in the air chamber above the free surface one can control the static pressure in the entire circuit since it forms a closed system. In the present facility the air chamber is located above the settling chamber and is denoted by "K" in figure 1. A free surface is maintained in this chamber while filling the tunnel and the air pressure above the free surface is controlled by a compressor unit and a vacuum pump. It may be noted here that the present technique of pressure control for a tunnel facility of the present size is certainly not adequate. An improved method is being designed and will be incorporated in the circuit in the near future. It should also be mentioned here that the presence of the air chamber is not only necessary to control the pressure but is also necessary to absorb volume changes in the rest of the circuit due to cavitation.

9 Water treatment plant : The circulating water in the tunnel should be clear and free from suspended impurities. To achieve this a separate water treatment plant+ has been designed and installed near the main water tunnel building. The following operating criteria was used to design the water treatment plant.

Turbidity of raw water	:	Slightly below 20 ppm
Rate of flow through filter	:	95 liters/minute
Filter loading	:	81.5 liters/sq.meter/min.
Working pressure	:	6 to 9 meters head of water
Effluent quality	:	Turbidity of not more than 2 ppm on the silica scale.

The main water supply from an Institute well is connected to an underground sump of capacity 22.7 cubic meters. The raw water is pumped to the filter unit by a centrifugal pump of one horse power capacity. The filtered water is stored in another underground sump of 45.4 cubic meters capacity. The filtered water is then pumped to the tunnel circuit by a centrifugal pump of twenty horse power capacity. The schematic diagram illustrating the filter plant with its accessories is shown in figure 14.

+ Supplied by M/s Dore and Sesh Co., Bangalore, India.

The pressure filter unit comprises of a cylindrical tank of 1.2 meters diameter and about 2 meters high. At the bottom of the tank a brass perforated plate with 188 perforations is placed. Above this plate graded gravel and sand is packed alternatively to trap the suspended impurities in the raw water. After 8 to 10 hours of continuous filtering, the packed gravel and sand traps significant amounts of impurities and this can be cleared up by backwashing the system. To arrest colloidal and bacterial contents of the raw water an alum dosing is provided prior to entering the pressure filter tank. Crystalline alum is placed in a cast iron pot equipped with a quick closing lid. A stainless steel orifice plate is provided in the delivery line from the pump to the pressure filter tank. The pressure differential across the orifice plate is used to circulate the raw water through the pot containing alum. A heavy alum dosing is necessary only at the beginning stages to create a slimy layer called 'SCHMUTZDECKE' on the pressure filter bed. This layer has the property of arresting the colloidal and bacterial germs. Once the layer has been formed the alum dosage can be reduced. In the present filter plant a stainless steel needle valve is provided at the outlet of the alum pot to control the dosing rate.

10 Photographic accessories : Photography has become an important aspect of studying cavitation phenomenon. The present facility has at its disposal equipment which can be used to take single flash photographs and also a high speed camera which can take photographs upto 8,000 frames per second. In addition, a photography lab is housed in the water tunnel building where development and printing work can be handled including processing of black and white motion picture films.

For single flash photography and cavitation observational purposes a phillips model PR 9108 with flash torch model PR 91117B/03 is available. The maximum flashing rate possible is 500 flashes per second. The stroboscope can be operated under single flash mode and the flashing can be controlled from external closure of a contact, like in a camera. The maximum intensity available is 2.25 watt sec. and at this intensity the exposure time is of the order of fifteen microseconds measured at the half peak points. This exposure is short enough to freeze any motion possible within the limitations of the tunnel velocity range.

For motion picture studies, a Fastax WF-2 camera is available with all its supporting equipment like the power supply, the high powered illuminating lamps etc. As noted earlier the maximum framing rate possible is 8,000 frames per second. Normally 16mm 100 foot length film is used. The high speed camera can be used under steady light illumination and also the camera shuttering can be synchronized with the flashing of a stroboscope. The latter technique can be used to study transient phenomenon with extremely short duration exposure per frame.

TABLE 1 - COMPARISON OF IISC-HSWT WITH

	CALIF. INST. OF TECH. (PASADENA) HIGH SPEED WATER TUNNEL	PENN STATE UNIV. (STATE COLLEGE) ORL GARFIELD THOMAS WATER TUNNEL
Construction period	1942-1947	1947-1951
Type of circuit	closed	closed
Purpose	Underwater bodies	Underwater bodies and propellers
Working Section Type	Closed jet	Closed jet
Diameter (in)	14	48
Velocity (ft/sec.)	100	80
Contraction Ratio	18	9
Resorber	Yes	No
Pressure Control Range Min (atm)	0.1	0.2
Max (atm)	7.5	4.0
Temperature Control	Yes	Yes (350 ton refrig.)
Main Circulating System Pumping unit	Prop. pump	Vari. Pitch prop.
Drive unit Type	Shunt would dc	Wound Rotor inductor
HP	350	2000
Speed Control	CIT electromech. control of motor field (feedback)	Kraemer
Force balance	3-component (hydraulic + strain guage)	6-component (strain guage)
Test object specs. Diameter (in.)	2 (standard test body)	8 (powered models)
Max. Power (HP)		70 (models with counter rotating props.)

SOME MAJOR CAVITATION RESEARCH CIRCUITS

ADMIRALTY RESEARCH LAB. (TEDDINGTON ENGLAND) 30-in WATER TUNNEL	NATIONAL PHYSICAL LAB. (TEDDINGTON ENGLAND) 44 in. WATER TUNNEL	NAVALSHIP RESEARCH AND DEVELOPMENT CENTER (WASHINGTON D.C.) 36 in. WATER TUNNEL	INDIAN INSTITUTE OF SCIENCE (BANGALORE, INDIA) HIGH SPEED WATER TUNNEL
1951-1954	1956-1959	1959-1962	1964-1968
closed	closed	closed	closed
Underwater bodies	Propeller testing	Underwater bodies and propellers	Underwater bodies
Closed jet and slotted walls	Closed jet	Open jet and closed jet	Closed jet
30	44	36	15
60	50	85	100
10	7.4	9	16
Yes	Yes (deep circuit)	Yes	Yes (Horizontal)
0.1	0.1	0.1	0.34
3.0	6.0	4.0	2.5
Yes	Yes (refrig.)	Yes (95-ton refrig.)	No
Propeller (Pitch adjustable when stationary)	Vari-Pitch Prop.	Vari-Pitch Prop.	Prop. Pump
dc	dc	Synch. motor with eddy current coupling	Wound rotor inductor
850	850	3500	600
Ward Leonard	Electronic control on dc motor speed	Electronic feedback system	AEI liquid controller
3-component (strain gauge inside model)	Thrust and Torque (swinging frame dc dyn.)	Thrust and torque (strain gauge)	None
10 (powered models)	12 to 24 (prop. clian.)	27 in (open), 18 in (closed)	2
200	300	1000 (to each of two model prop. shafts)	

LIST OF FIGURE CAPTIONS

Figure 1 : Schematic diagram of the 381 mm Indian Institute of Science High Speed Water Tunnel

Figure 2 : Geometrical details of the hemispherically nosed test body

Figure 3 : Incipient and developed cavitation on a hemispherical nosed body. (a) Test section with model and strut under supercavitating conditions (b) Bubble cavitation at inception. (c), (d) and (e) developed stages of cavitation with reduction in σ below σ_i.

Figure 4 : Variation of incipient and desinent cavitation index with tunnel velocity.

Figure 5 : Comparison of present data with previous findings at the CIT and ORL water tunnel facilities

Figure 6 : Pressure distribution on a hemispherical nosed body under non-cavitating conditions

Figure 7 : Photographs of certain components and supporting equipment of the tunnel facility
(a) Building accommodating the High Speed Water Tunnel (b) Upper leg showing the diffuser, test section, contraction cone and settling chamber. Also seen is the pressure control chamber marked as K in figure 1. (c) Resorber section above the floor level (d) 600 H.P. induction motor (e) Control equipment of the motor. On far side is the oil circuit breaker and on near side is the liquid control regulator.

Figure 8 : Certain geometrical details of the test section

Figure 9 : Geometrical details of the horizontal resorber. Baffle locations are also shown.

Figure 10 : Side view of the resorber showing cross hatched welding of the I-beam section to strengthen the resorber side flat plates.

Figure 11 : Geometrical shape of the contraction cone. Note X and D are in inches (1 inch = 25.4 mm)

Figure 12 : Geometrical shape of the turning vane used in all bends except in the pump. Note all dimensions are in millimeters.

Figure 13 : Characteristics of the main four bladed circulating pump

Figure 14 : Schematic diagram water filter plant and its accessories. Note all dimensions are in millimeters.

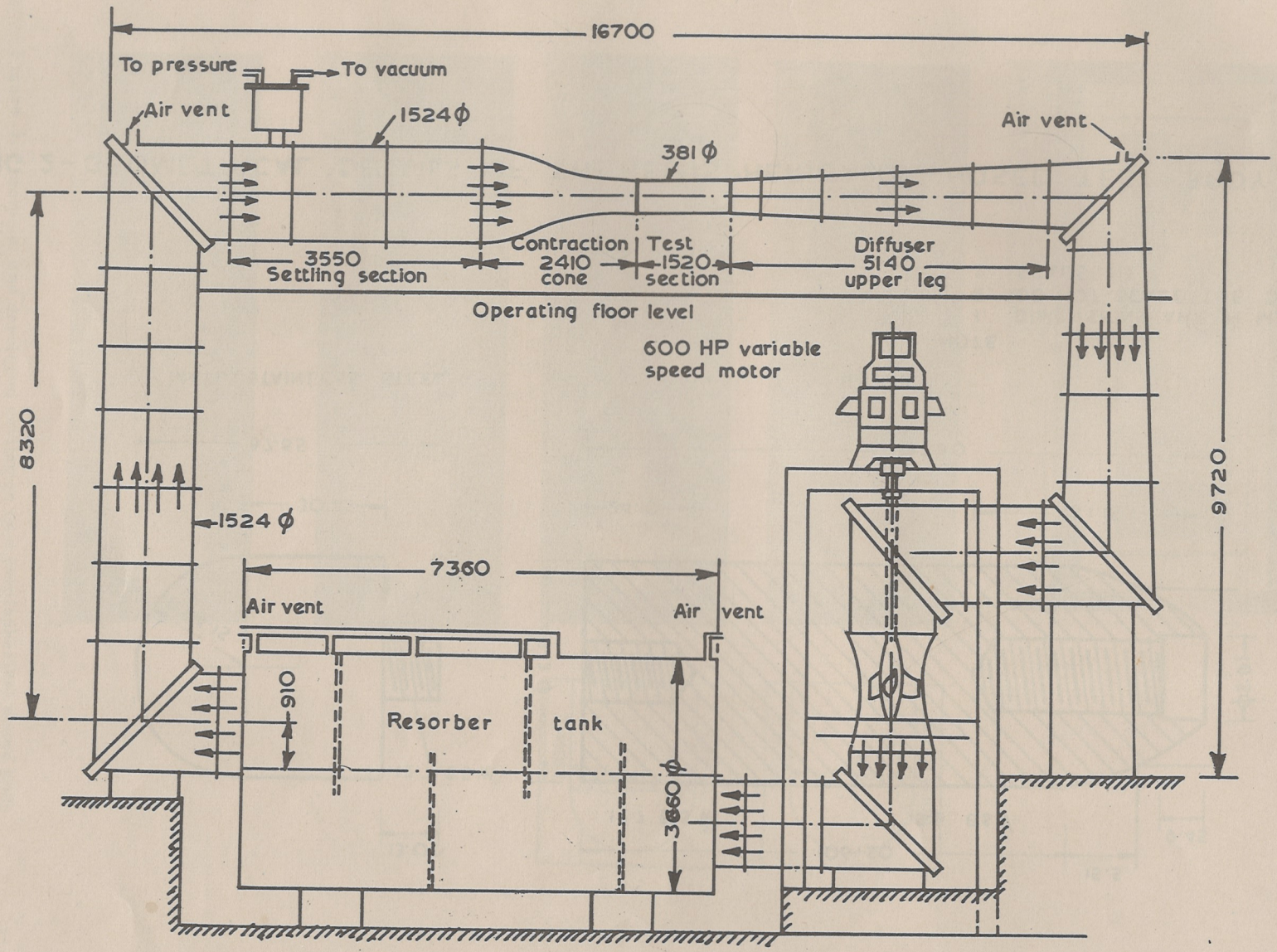

FIG.1 : SCHEMATIC DIAGRAM OF THE 381 mm INDIAN INSTITUTE OF SCIENCE HIGH SPEED WATER TUNNEL

1524
381

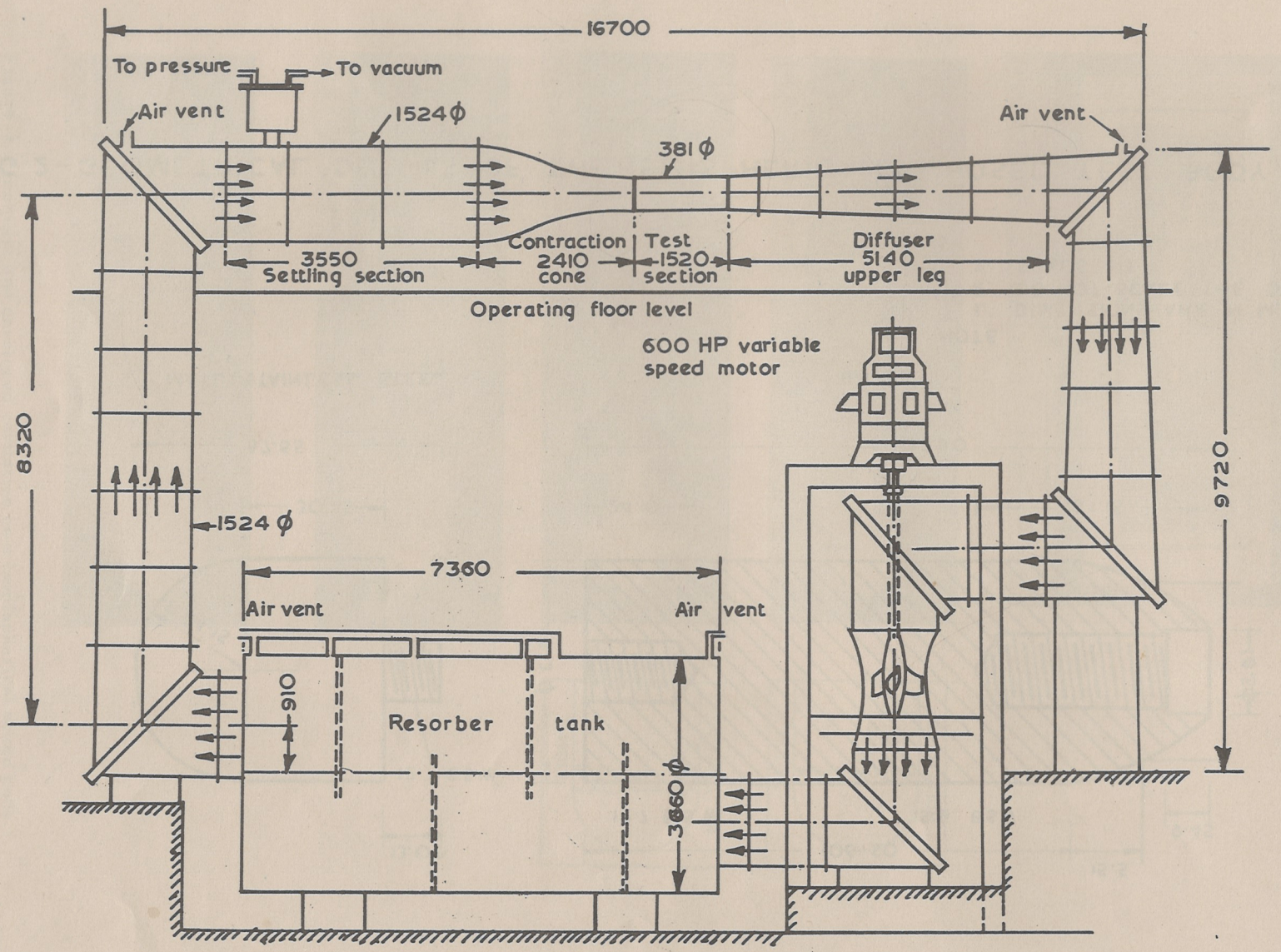

FIG.1 : SCHEMATIC DIAGRAM OF THE 381 mm INDIAN INSTITUTE OF SCIENCE HIGH SPEED WATER TUNNEL

1524
381

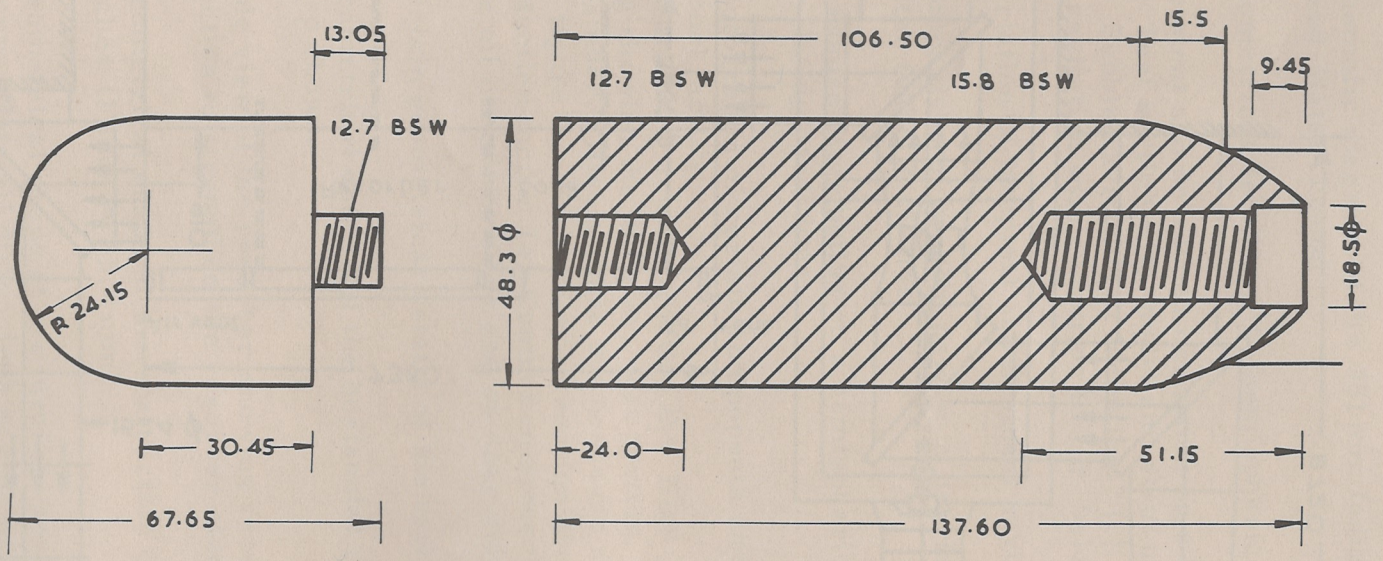

NOTE

1. DIMENSIONS ARE IN M.M.
2. DO NOT SCALE THE DRAWING
3. SCALE 1:1

FIG.2 - GEOMETRICAL DETAILS OF THE HEMISPHERICALLY - NOSED TEST BODY.

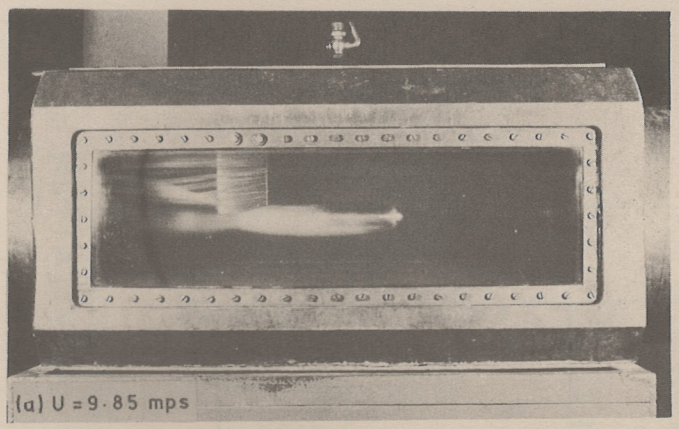

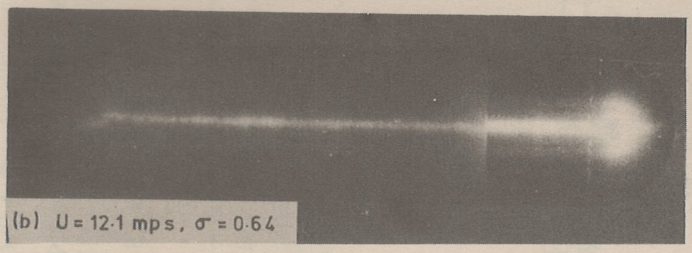

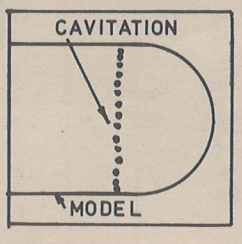

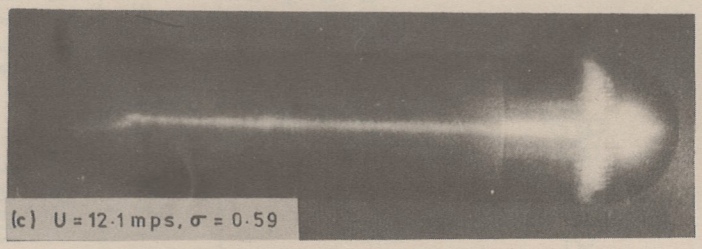

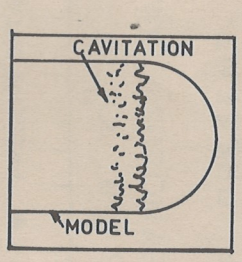

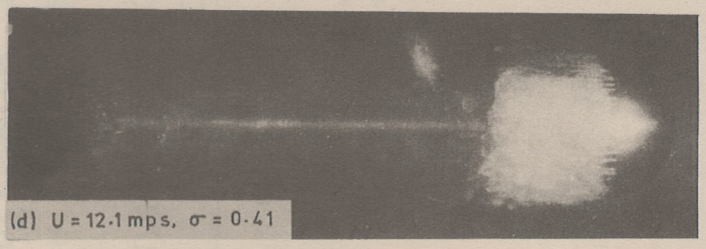

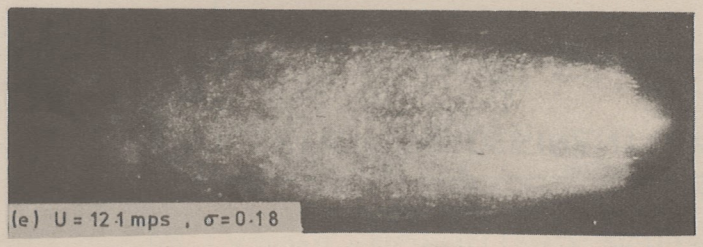

Figure 3. **Incipient and developed cavitation on a hemispherical nosed body.**
(a) Test section with model and strut super-cavitating conditions.
(b) Bubble cavitation at inception.
(c), (d) and (e) Developed stages of cavitation with reduction in σ below σ_i .

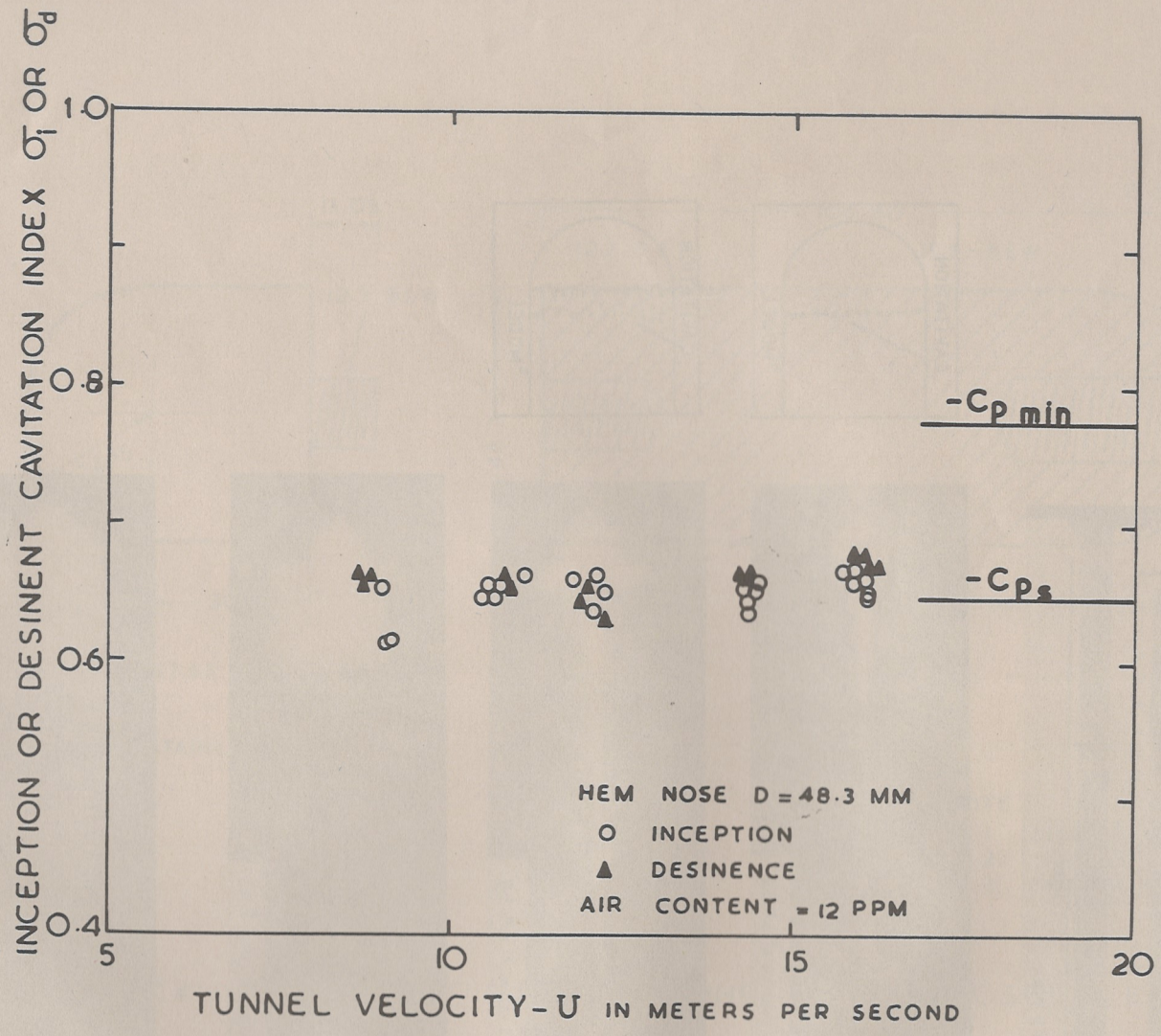

FIG. 4 - VARIATION OF INCIPIENT AND DESINENT CAVITATION INDEX WITH TUNNEL VELOCITY.

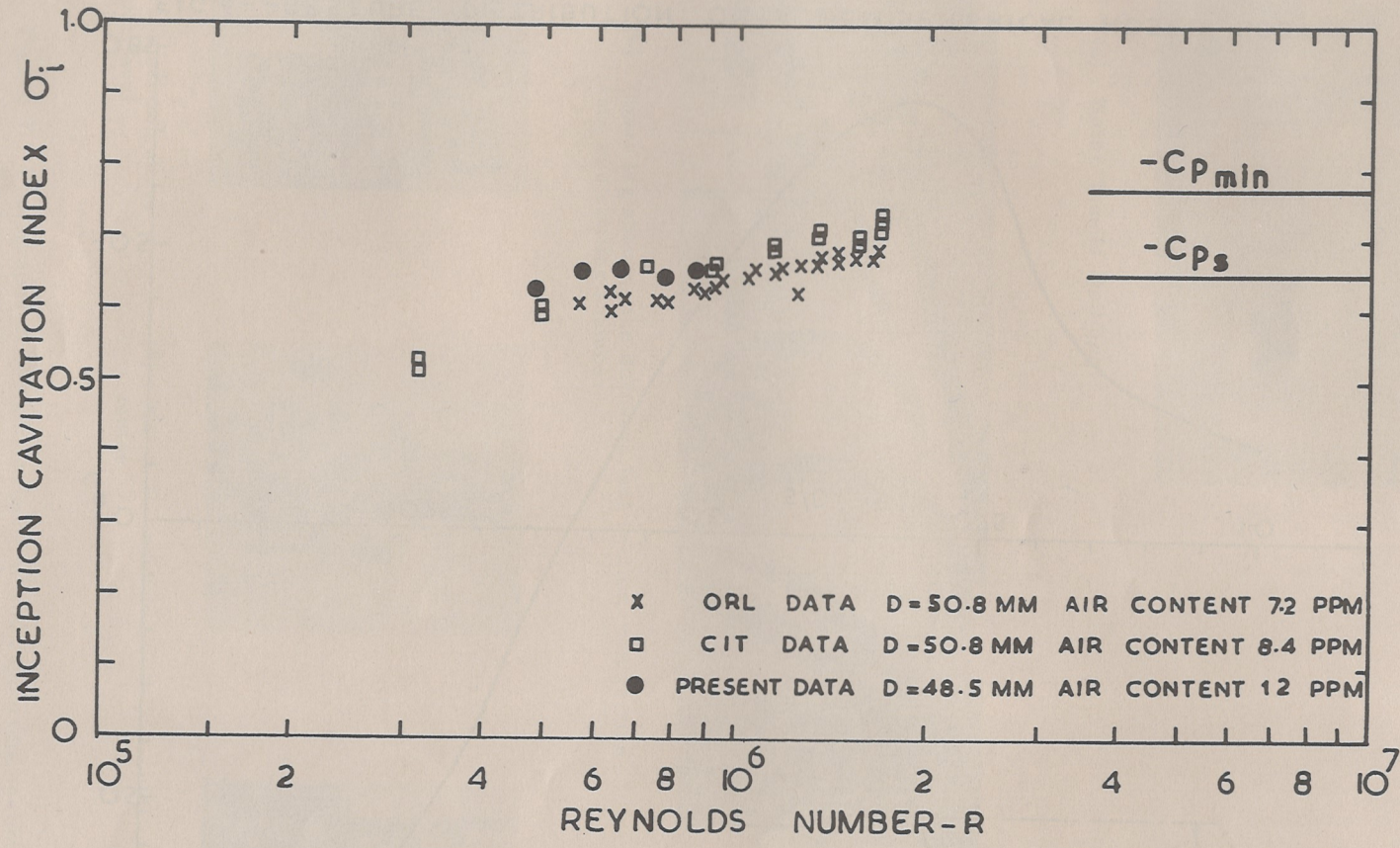

FIG. 5 - COMPARISION OF PRESENT DATA WITH PREVIOUS FINDINGS AT THE CIT AND ORL WATER TUNNEL FACILITIES

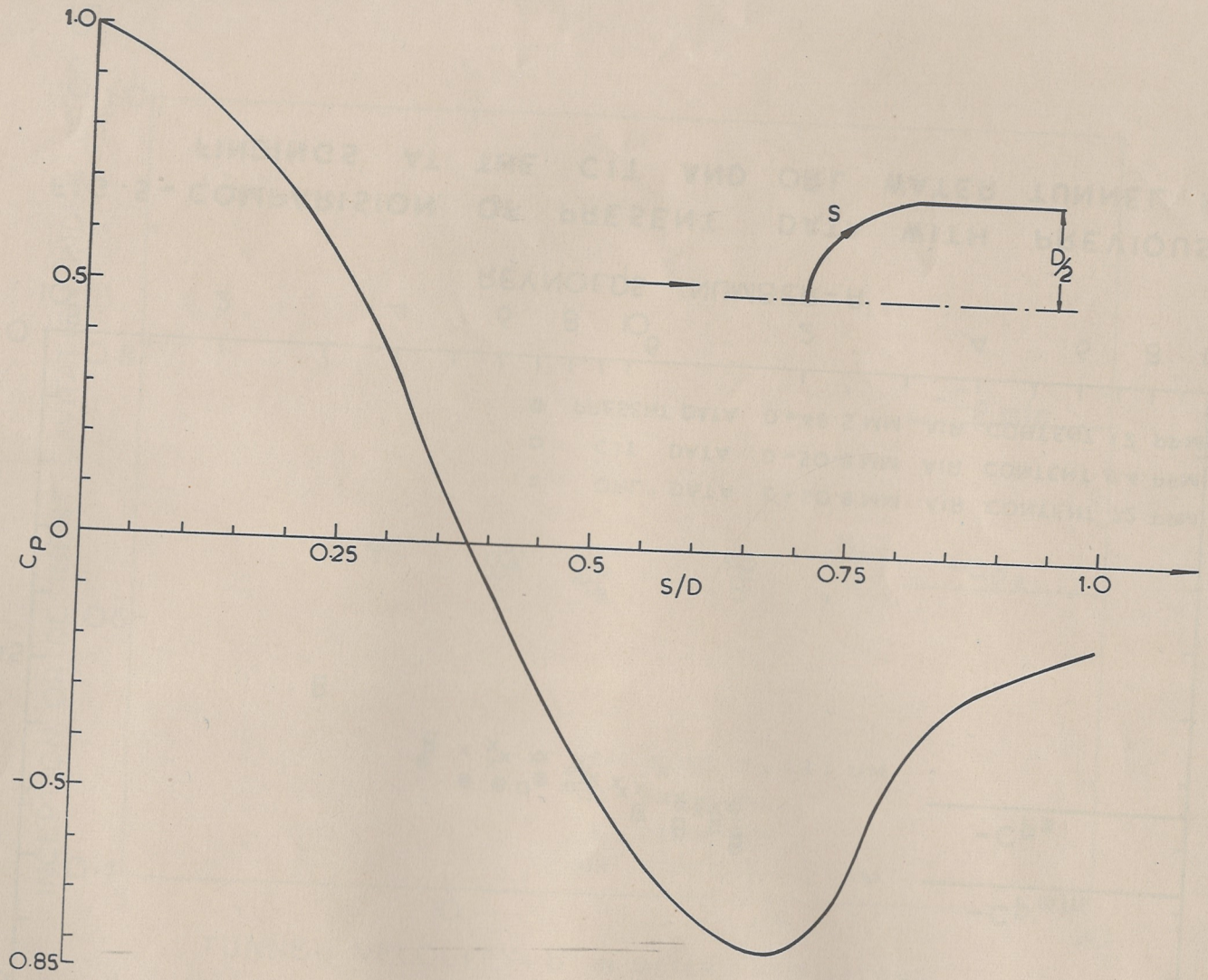

FIG.6 - PRESSURE DISTRIBUTION ON A HEMISPHERICAL NOSED BODY UNDER NON-CAVITATING CONDITIONS.

(a) Water Tunnel Building

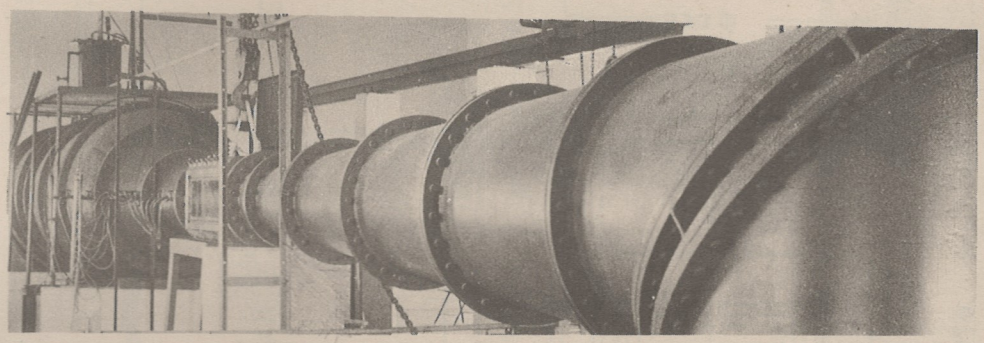

(b) Upper leg showing the diffuser, test section, contraction cone and settling chamber

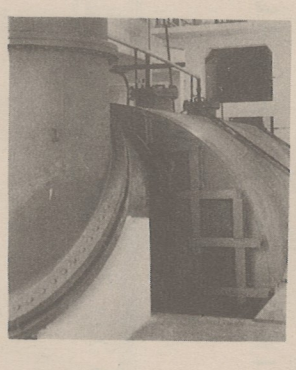

(c) Resorber section above the floor level

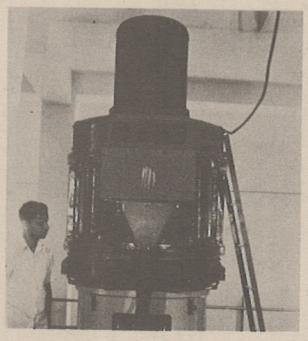

(d) 600 H.P. induction motor

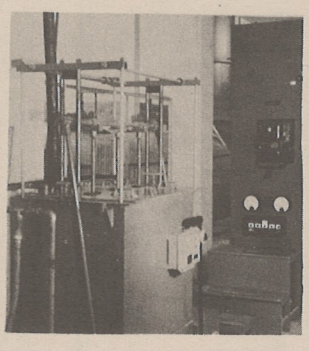

(e) Control equipment of the motor

Figure 7. Photographs of certain components and supporting equipment of the tunnel facility. Note in (e) the oil circuit breaker is on far side and the liquid control regulator is on the near side.

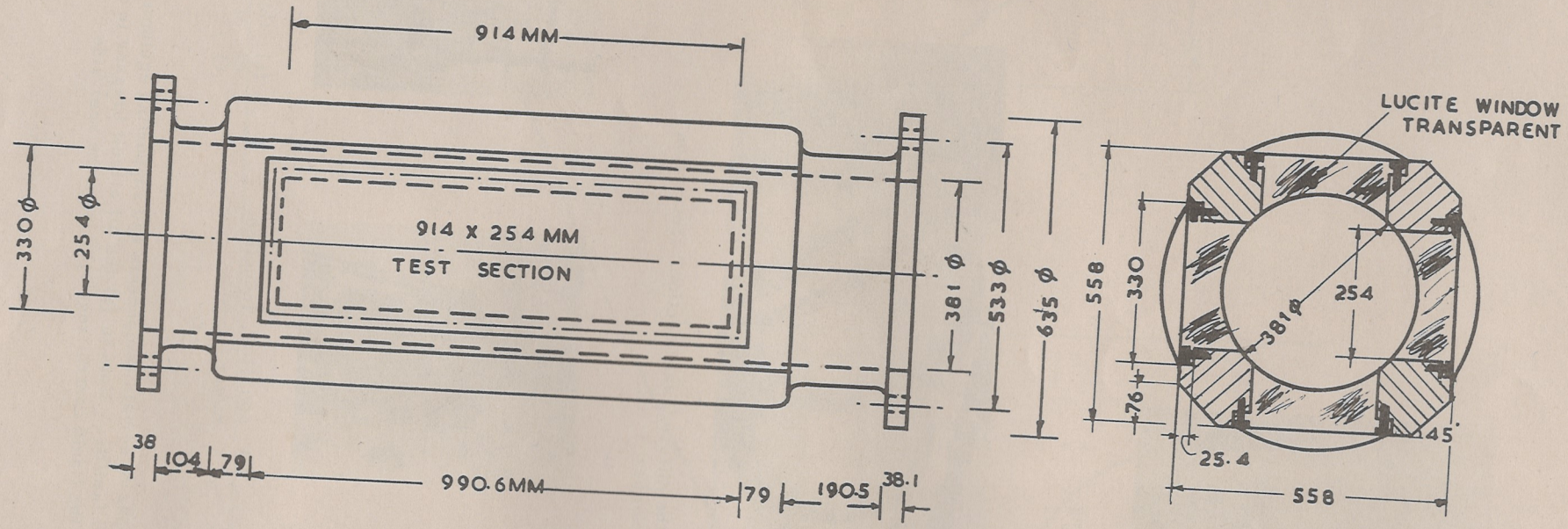

FIG.8. CERTAIN GEOMETRICAL DETAILS OF THE TEST SECTION.

Model - 556 mm.

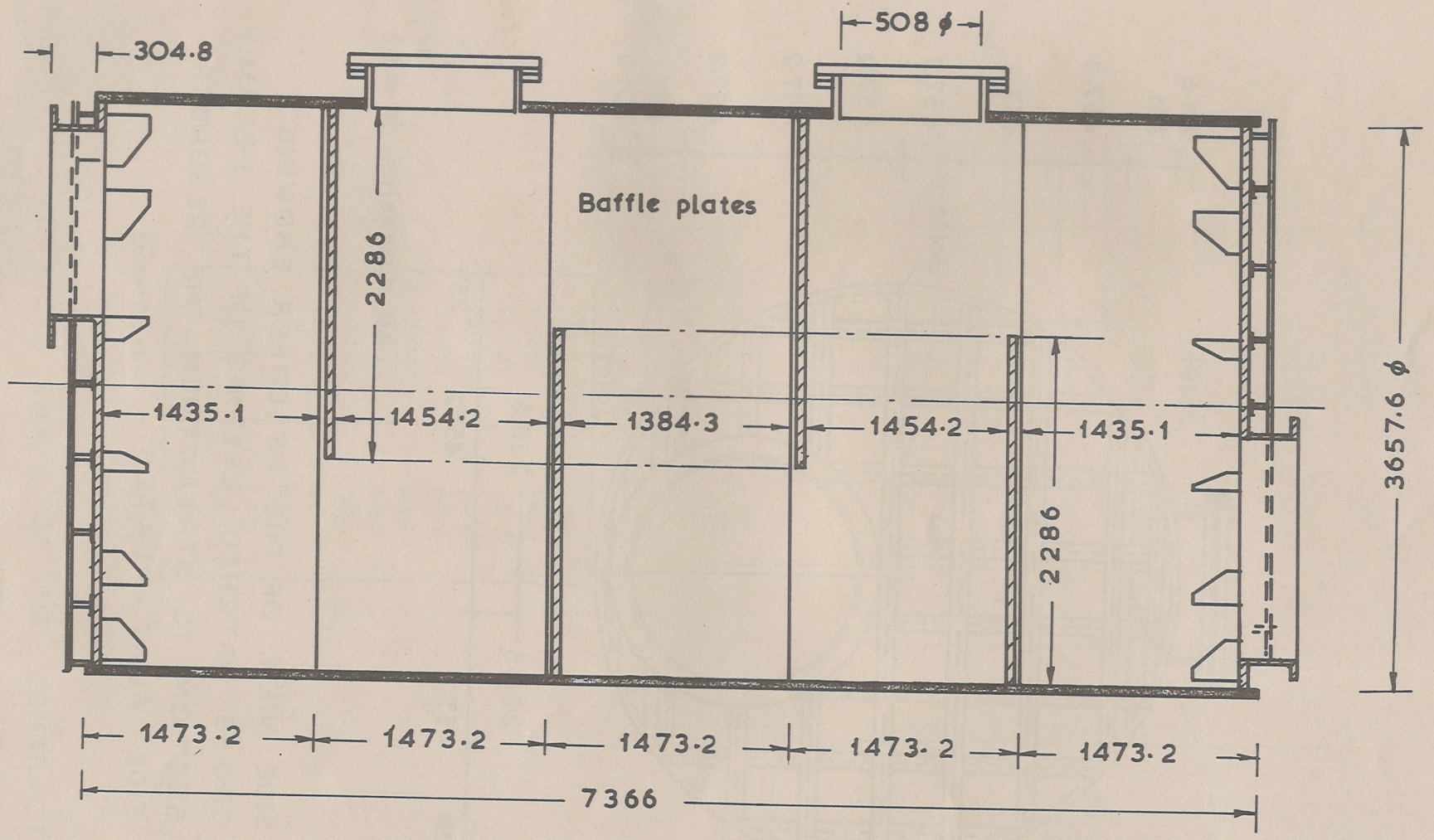

FIG.9- GEOMETRICAL DETAILS OF THE HORIZONTAL RESORBER. BAFFLE LOCATATIONS ARE ALSO SHOWN.

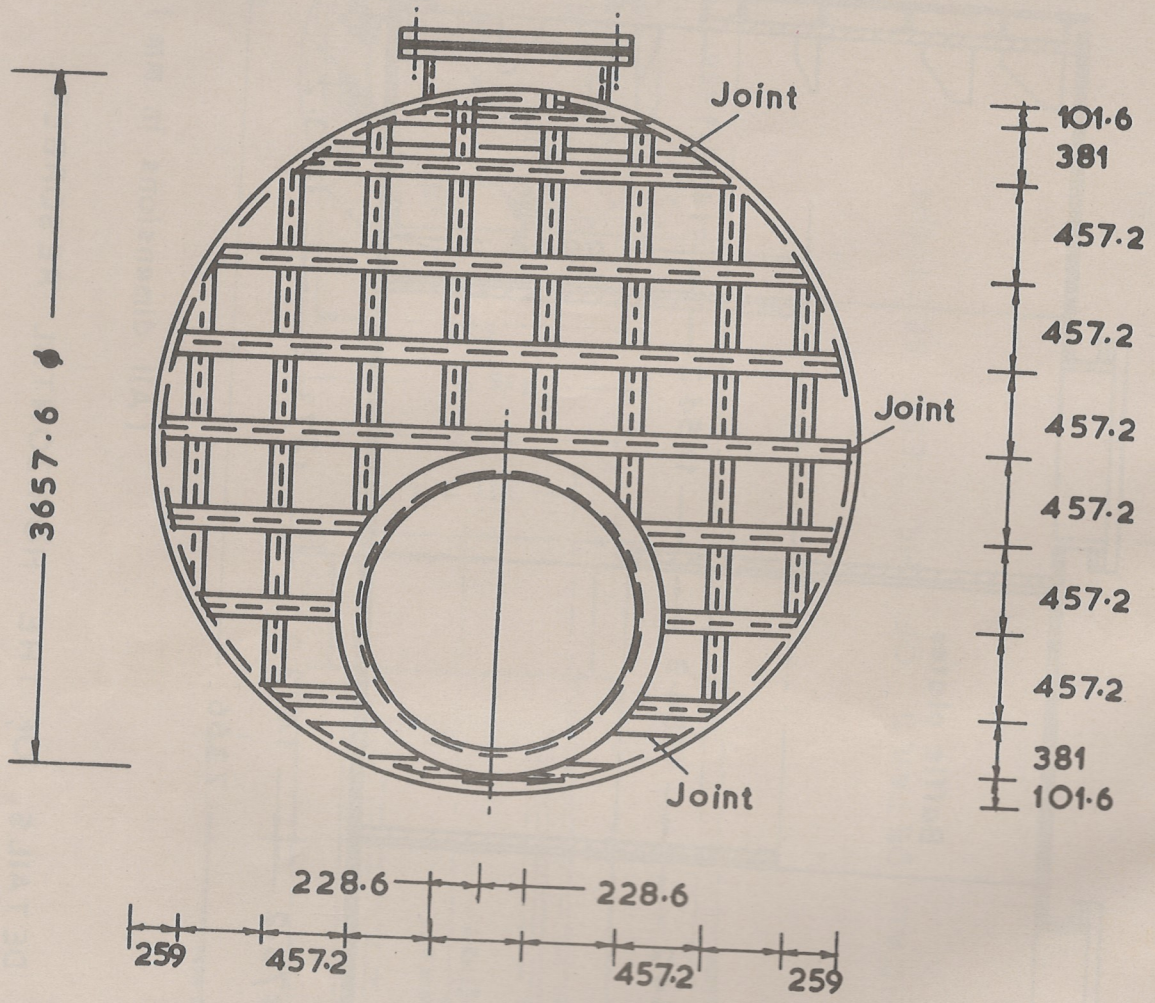

(All dimensions in mm)

FIG.10- SIDE VIEW OF THE RESORBER SHOWING CROSS HATCHED WELDING OF THE I-BEAM SECTION TO STRENGTHEN THE RESORBER SIDE FLAT PLATES.

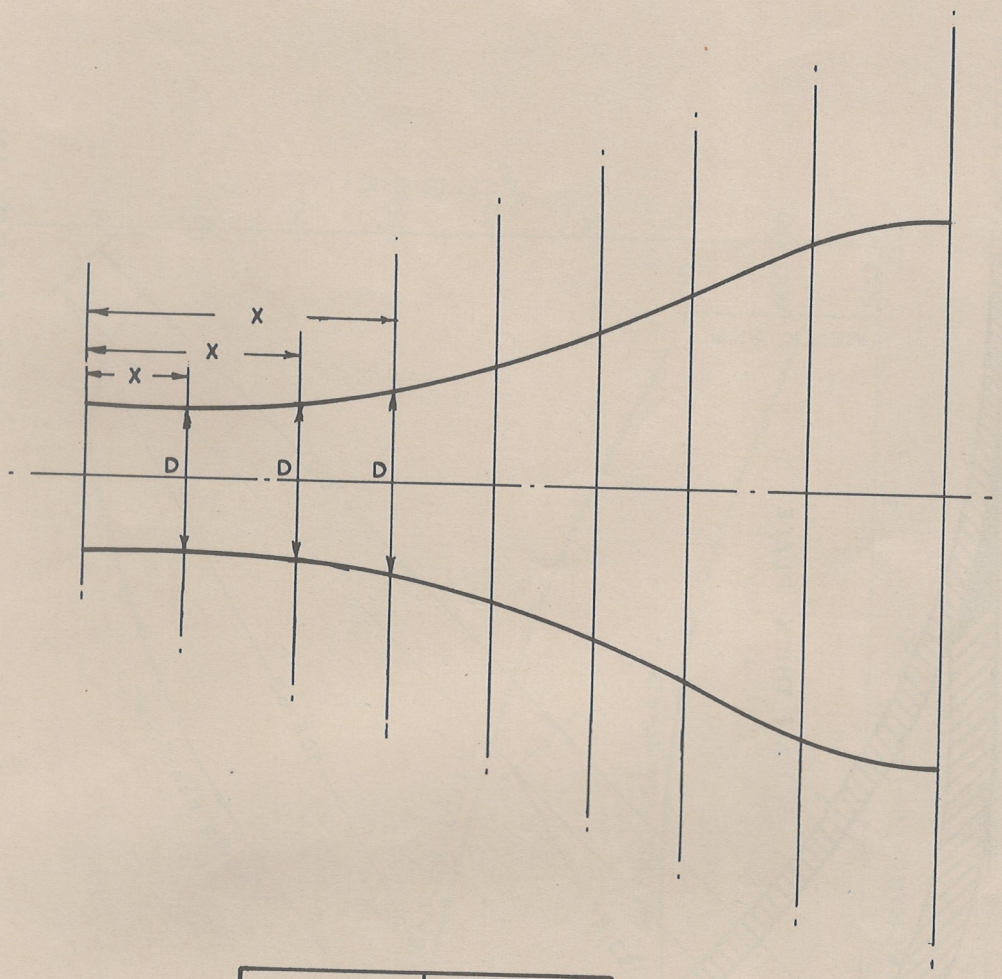

X	D
11·214	15·6
16·581	16·2
23·169	17·4
33·693	20·4
45·081	25·2
50·310	30·0
56·010	32·4
60·18	36·0
66·63	43·2
70·98	48·0
79·29	58·2
94·23	60·0

Dimensions in inches

FIG. 11. GEOMETRICAL SHAPE OF THE CONTRACTION CONE.

Note. X and D are in inches
(1 inch = 25·4 mm)

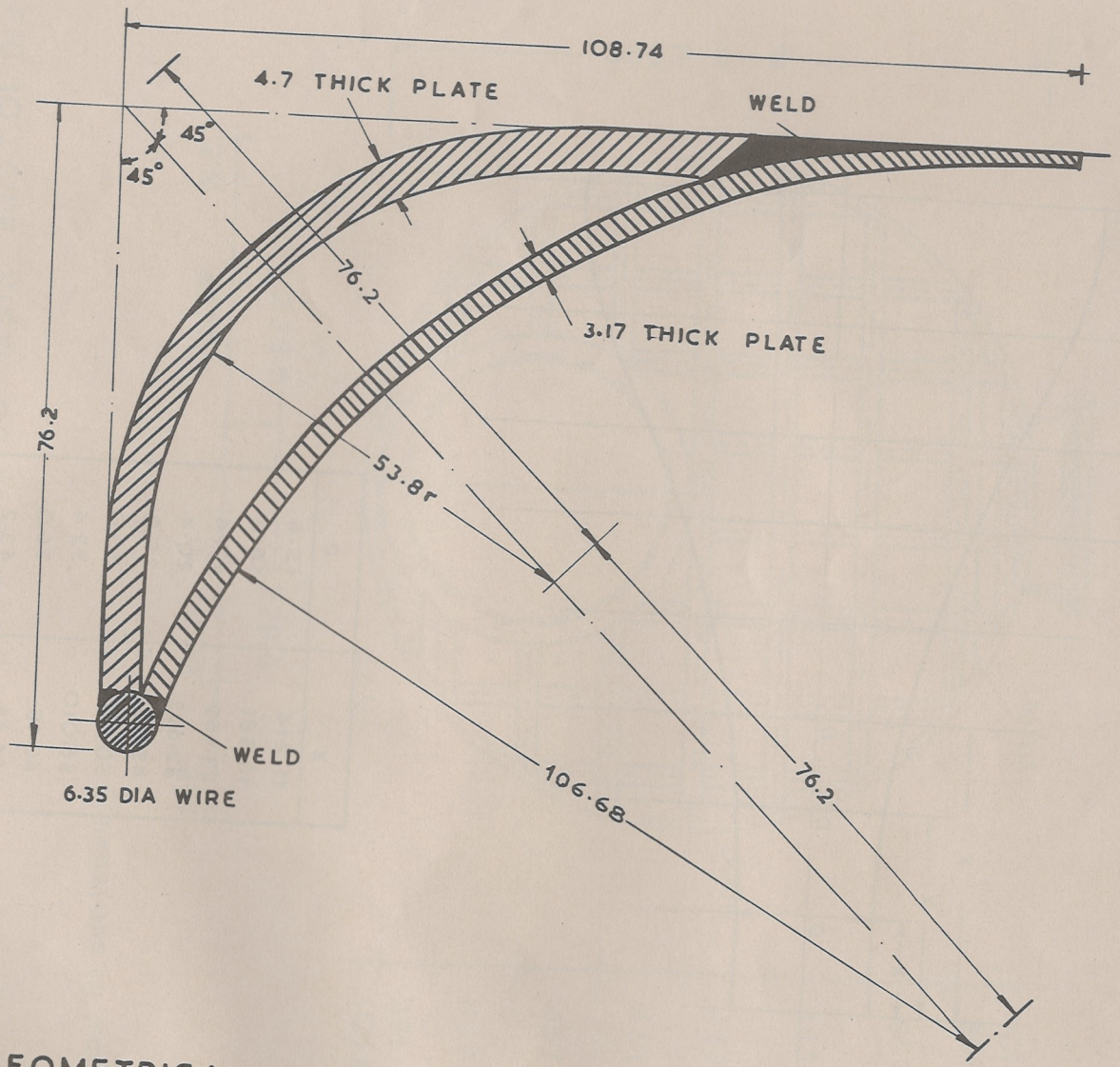

FIG.12 - GEOMETRICAL SHAPE OF THE TURNING VANE USED IN ALL BENDS EXCEPT IN THE PUMP.

Note : All dimensions are in mm

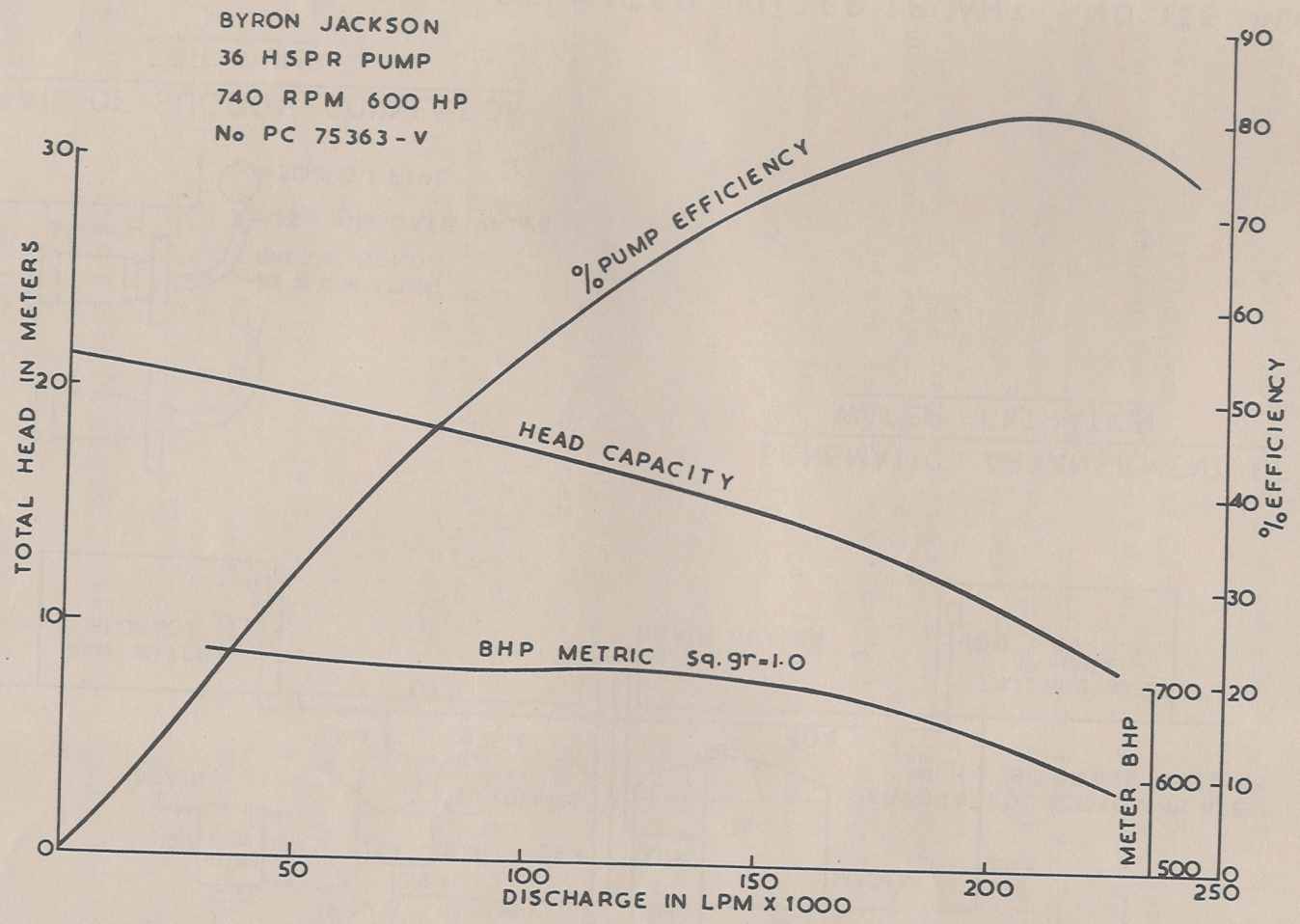

FIG.13- CHARACTERISTICS OF THE MAIN FOUR BLADED CIRCULATING PUMP.

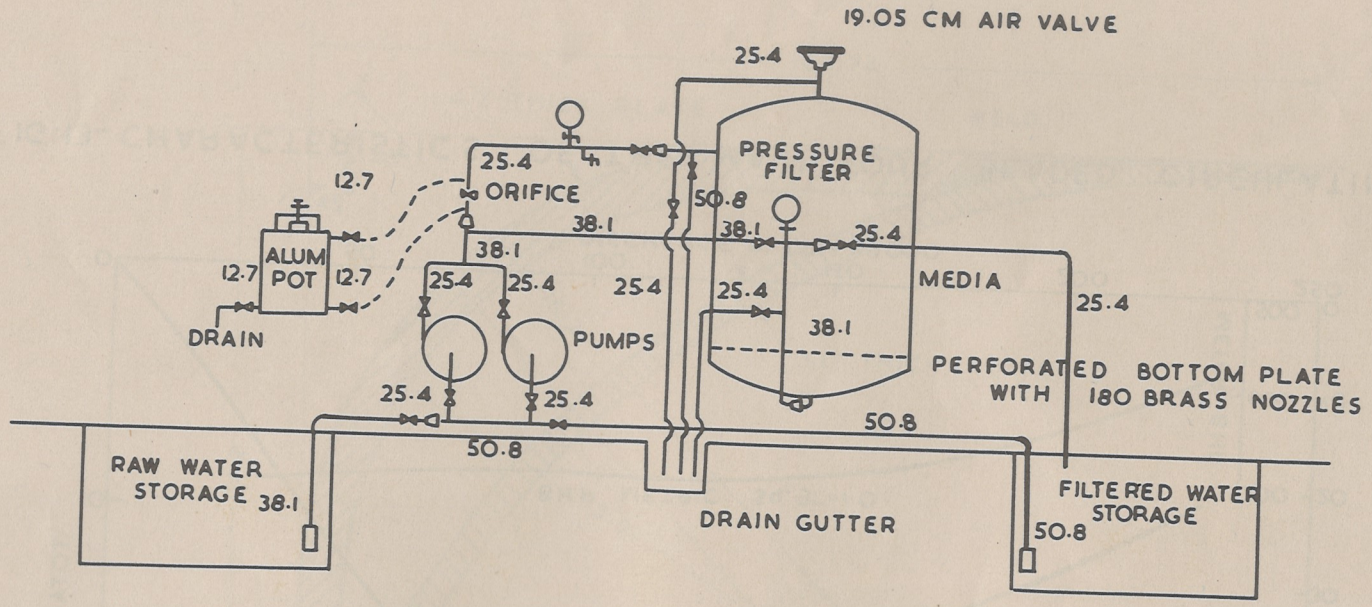

SCHEMATIC ARRANGEMENT OF WATER FILTRATION

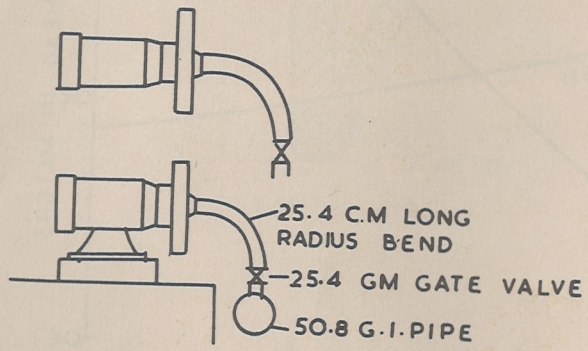

DETAIL OF SUCTION CONNECTION FOR PUMP

FIG.14 – SCHEMATIC DIAGRAM OF WATER FILTER PLANT AND ITS ACCESSORIES.

Note : All dimensions are in mm.

REFERENCES

1 Plesset, M.S., "Cavitation State of Knowledge", ASME, New York, p.15, 1969.

2 Plesset, M.S., "The Dynamics of Cavitation Bubbles", Journal of Applied Mechanics, Trans. of the ASME, Vol.16, pp.277-288, September 1949.

3 Arakeri, V.H. and Acosta, A.J., "Viscous Effects in the Inception of Cavitation on Axisymmetric Bodies", Journal of Fluids Engineering, ASME, Vol.95, Sec.1, No.4, pp.519-528, 1974.

4 Seetharamaiah, K. and Nanjundaswamy, Y.S., "Design of 15" Cavitation Tunnel", Presented at the Annual Research Committee meeting of CBIP, Simla 1963. (Also see Annual report of Civil and Hydraulic Engg. Rept. 1963).

5 Nanjundaswamy, Y.S., "On the Design of a two Dimensional Contracting Channel", Journal of Aero Space Sciences, 1961.

6 Nanjundaswamy, Y.S. "A note on the Design of a two Dimensional Contracting Channel", Journal of Aero Space Sciences, February, 1962.

7 Acosta, A.J. and Hamaguchi, H., "Cavitation Inception on the I.T.T.C. Standard Head Form", CIT Report No. E-149.1, March 1967.

8 Parkin, B.R. and Holl, J.W., "Incipient - Cavitation Scaling Experiments for Hemispherical and 1.5 Calibre Ogive-Nosed Bodies", Report Nord 7958 - 264, Ordance Research Laboratory, Pennsylvania State University, February 1956.

9 Robertson, J.M. and Ross, D., "Effect of Entrance Conditions on Diffuser Flow", Trans ASCE, Vol.118, 1953, pp.1068-1097.

10 Gates, E.M., "The Influence of Freestream Turbulence, Free Stream Nuclei Populations and a Drag - Reducing Polymer on Cavitation Inception on Two Axisymmetric Bodies", CIT Report No. Eng.183-2, April 1977.

11 "Cavitation Research Facilities and Techniques", ASME Publication, New York, 1964.

12 Thwaites, B., "On the Design of Contractions for Wind Tunnels", R and M No.2278, ARC (British), March 1946.

13 Klein, S.J., et al., "The Design of Corners in Fluid Channels", Canadian Journal of Research, Vol.3, July 1930, pp.272-285.

14 Ripken, J.F., "Design Studies for a Closed Jet Water Tunnel", Technical Report No.9, Series B, University of Minn., SAFHL, August 1951.